On the Measurement of Total Radiated Power in Uncalibrated Reverberation Chambers

Hans Georg Krauthäuser, *Member, IEEE*

***Abstract*—A novel experimental procedure to measure the total radiated power of an equipment under test (EUT) placed in a reverberation chamber (RC) is presented. In contrast to the well-established method of the IEC 61000-4-21, this new procedure does not rely on information obtained during the empty chamber calibration or the calibration with the EUT in place. Thus, the method is simpler, faster, and may have a smaller uncertainty budget.**

***Index Terms*—Emission measurement, IEC 61000-4-21, mode-stirred chamber, reverberation chamber (RC), total radiated power.**

I. Introduction

REVERBERATION chambers (RCs) are well-established environments to perform electromagnetic susceptibility and emission measurements. Since August 2003, the measurement procedures have been standardized in the IEC document IEC 61000-4-21 [1].

In this paper, the measurement of the total radiated power of an equipment under test (EUT) in an RC will be addressed. There is an ongoing discussion whether electromagnetic compatibility (EMC) emission limits for very high frequencies should refer to total radiated power or—as traditionally—to maximum electric field strength in a certain distance, see, e.g., [2]–[6]. The aim of this paper is not to vote for either of this possibilities. Rather, it is only about the introduction of a new measurement method, which seems to be not only simpler and faster but also equally accurate.

II. Theory

One of the most important quantities in the study of RCs is the quality factor Q [7], [8]. The general definition of Q is 2π times the ratio of the energy stored to the energy dissipated per cycle [9]. Thus

$$Q = \frac{\omega U_s}{P_d} = \frac{\omega U_s}{P_t}. \tag{1}$$

Here, $\omega = 2\pi f = 2\pi c/\lambda$ is the cycle frequency, U_s is the stored energy, P_d is the dissipated power, and P_t is the power transmitted to the chamber. The dissipated and the transmitted power are equal because steady-state conditions are assumed, i.e., $P_d = P_t$.

Manuscript received May 31, 2006; revised October 26, 2006. This work was supported in part by the Deutsche Forschungsgemeinschaft (DFG) under Contract FOR417-T5.

The author is with the Department of Electrical Engineering and Information Technology, Otto-von-Guericke-University Magdeburg, D-39106 Magdeburg, Germany (e-mail: hgk@ieee.org).

Digital Object Identifier 10.1109/TEMC.2007.897122

Either boundary, frequency, or spacial averaging has to be applied to achieve statistical homogeneous and isotropic fields in the RC. Typically, the boundary conditions are changed using a mechanical "mode stirrer." Denoting averaged quantities by $\langle\cdot\rangle$, (1) can be rewritten for the use in RCs as

$$\langle Q\rangle = \frac{\omega\langle U_s\rangle}{\langle P_d\rangle} = \frac{\omega\langle U_s\rangle}{\langle P_t\rangle}. \tag{2}$$

The averaged stored energy $\langle U_s\rangle$ is related to the averaged energy density $\langle W\rangle$ by

$$\langle U_s\rangle = \langle W\rangle V \tag{3}$$

where V is the chamber volume.

Combining (2) and (3) leads to an expression for the averaged energy density

$$\langle W\rangle = \frac{\lambda\langle Q\rangle\langle P_t\rangle}{2\pi c V}. \tag{4}$$

Now, a lossless and matched receiving antenna in the working volume of the RC is considered. The averaged received power $\langle P_r\rangle$ at this antenna is given by the product of the (scalar) averaged power density $\langle S_c\rangle = c\langle W\rangle$ and the averaged effective area of the receiving antenna $\langle A_e\rangle$ [10]

$$\langle P_r\rangle = \langle S_c\rangle\langle A_e\rangle = c\langle W\rangle\langle A_e\rangle. \tag{5}$$

The average effective area of any antenna located in an RC is equal to the average effective area of an isotropic antenna $\lambda^2/4\pi$ corrected by the polarization mismatch factor p_m [11], [12]

$$\langle A_e\rangle = p_m\frac{\lambda^2}{4\pi} \tag{6}$$

$$= \frac{\lambda^2}{8\pi}. \tag{7}$$

The polarization mismatch factor is equal to 1/2 for any antenna in an ideal RC [13].

Applying (4) and (7) to (5) finally yields

$$\langle P_r\rangle = c\frac{\lambda\langle Q\rangle\langle P_t\rangle}{2\pi c V}\frac{p_m\lambda^2}{4\pi} = \frac{p_m\lambda^3\langle Q\rangle}{8\pi^2 V}\langle P_t\rangle \tag{8}$$

or

$$\langle P_t\rangle = \frac{8\pi^2 V}{p_m\lambda^3\langle Q\rangle}\langle P_r\rangle. \tag{9}$$

For the case of a real receiving antenna, the measured power is reduced by ohmic losses in the antenna—expressed by the antenna efficiency η_r ($\in [0,1]$)—and due to the mismatch of the antenna port [8]. The latter is given by $(1-|S_{22}|^2)$ ($\in [0,1]$), where S_{22} is the reflection coefficient of the antenna "looking into" the antenna port. Taking this effect into account leads to

$$\langle P_t \rangle = \frac{8\pi^2 V}{p_m \eta_r (1-|S_{22}|^2)\lambda^3 \langle Q \rangle} \langle P_r \rangle. \tag{10}$$

The antenna efficiency is difficult to measure. It is a common practice to assume

$$\eta_r = \begin{cases} 0.75, & \text{for log-periodic antenna} \\ 0.9, & \text{for horn antenna.} \end{cases} \tag{11}$$

Measurements of the antenna mismatch can be affected by the antenna losses. For "not too bad" matched antennas, the antenna mismatch factor is commonly neglected, i.e., $(1-|S_{22}|^2) = 1$. Thus, for well-matched antennas, the following equation can be used:

$$\langle P_t \rangle = \frac{16\pi^2 V}{\eta_r \lambda^3 \langle Q \rangle} \langle P_r \rangle. \tag{12}$$

The power $\langle P_r \rangle$ is the received power at the antenna port. It is assumed that appropriate corrections for cable losses are applied to the measured data.

There are different possibilities for the experimental evaluation of (12). Whereas the two possibilities described in the IEC standard involve results from preceding calibration measurements, the new procedure presented later obtains all information within a single measurement.

A. IEC Procedures

The IEC standard 61000-4-21 lists two possibilities to obtain the total radiated power P_{rad} of the EUT.[1]

1) Based on the measurement of the averaged received power

$$P_{\mathrm{rad}} = \frac{\eta_T P_{\mathrm{AveRec}}}{\mathrm{CCF}}. \tag{13}$$

Here, P_{AveRec} is the averaged (over tuner positions) power at the receiving antenna port, and CCF is the chamber calibration factor defined as

$$\mathrm{CCF} = \left\langle \frac{P_{\mathrm{AveRec}}}{P_{\mathrm{input}}} \right\rangle_{\mathrm{antenna\,positions}}. \tag{14}$$

The chamber calibration factor is obtained from a EUT-calibration measurement. During this measurement, the EUT is in place but switched off. The RC is excited with a sine wave of averaged power P_{input} (average with respect to tuner positions) and the average power at the receiving antenna P_{AveRec} is recorded. $\langle\cdot\rangle_{\mathrm{antenna\,positions}}$ refers to the average with respect to different receiving antenna positions inside the working volume of the chamber (may be only one position).

2) Based on the measurement of the maximum received power

$$P_{\mathrm{rad}} = \frac{\eta_T P_{\mathrm{MaxRec}}}{\mathrm{CLF} \times \mathrm{IL}}. \tag{15}$$

Here, P_{MaxRec} is the maximum received power of the used tuner positions. The chamber loading factor is a combination of measurement results of the EUT calibration and the empty chamber calibration. The latter is performed after the construction of the chamber, after modifications, or—as a good practice—once in a year. The CLF is defined as

$$\mathrm{CLF} = \frac{\mathrm{CCF}}{\mathrm{ACF}} \tag{16}$$

where ACF is the antenna calibration factor, which is defined in the same way as the CCF but for the case of the empty chamber. The chamber insertion loss IL is obtained from the empty chamber calibration and is given by

$$\mathrm{IL} = \left\langle \frac{P_{\mathrm{MaxRec}}}{P_{\mathrm{input}}} \right\rangle_{\mathrm{antenna\,positions}}. \tag{17}$$

Eight different antenna positions are used during the empty chamber calibration.

Generally, the first method using P_{AveRec} should be preferred. The advantages are a lower uncertainty of the average compared to the maximum of the received power. Further, the results of the empty chamber calibration are not required for the calculation of the total radiated power.

Remarkably, the characteristics of the receiving antenna (polarization, efficiency, impedance mismatch) do not affect the results of the measurements. This becomes clear if (13) is reformatted (for one antenna position)

$$\frac{P_{\mathrm{rad,EUT}}}{P_{\mathrm{AveRec,EUT}}} = \frac{\eta_T P_{\mathrm{input,EUTCal}}}{P_{\mathrm{AveRec,EUTCal}}}. \tag{18}$$

The quantity $\eta_T P_{\mathrm{input,EUTCal}}$ is the radiated power during the EUT calibration *if* $P_{\mathrm{input,EUTCal}}$ is the power delivered to the antenna. The estimation of $P_{\mathrm{input,EUTCal}}$ is a problem since it is neither the forward power (because of impedance mismatch) nor the net power (forward minus backward). The latter is because the transmitting antenna also receives a certain amount of the chamber field that adds to the backward running power [8]. Typically, a well-matched antenna is assumed and the forward power is used.

B. New Procedure

In contrast to the IEC procedure discussed before, all information for the evaluation of (12) should be obtained from a single measurement, i.e., to measure $\langle P_r \rangle$ and $\langle Q \rangle$ simultaneously. The key idea is based on a measurement procedure for $\langle Q \rangle$ that has been published previously [14], [15].

1) Measurement of $\langle Q \rangle$: In order to measure the average quality factor $\langle Q \rangle$ (with the EUT in place), the experimental setup depicted in Fig. 1 is used.

The chamber is excited with a pulse modulated sine from the signal generator using the transmitting antenna (Tx). Both the "on" and the "off" time of the signal have to be large compared to the chamber time constant τ, which, in turn, is given by the chamber quality factor by $\tau = \langle Q \rangle / \omega$. The estimation of an upper bound of the time constant is uncritical. For the used RC, it can be approximated generously, e.g., to 20 μs. Typically, an "on" time of 50 μs and an "off" time of 150 μs is used.

The power at the receiving antenna is measured using a spectrum analyzer in zero span mode. In zero span mode, the video

[1]The notation from the IEC standard is used.

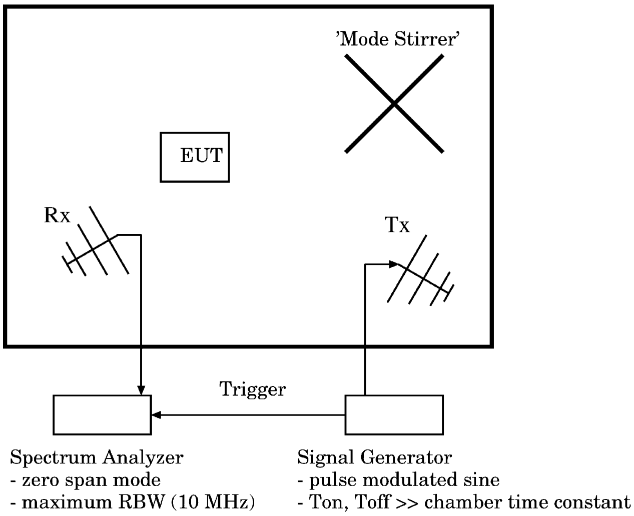

Fig. 1. Experimental setup to measure the quality factor $\langle Q\rangle$.

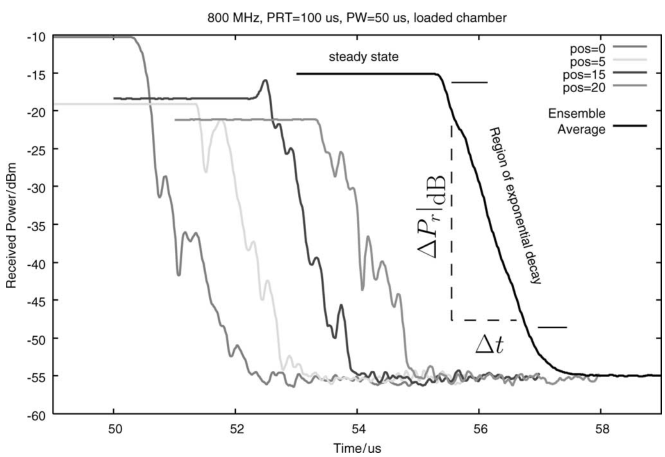

Fig. 2. Typical traces of the received power for different tuner positions. After the exiting signal is switched off, an exponential decay can be observed in the averaged trace.

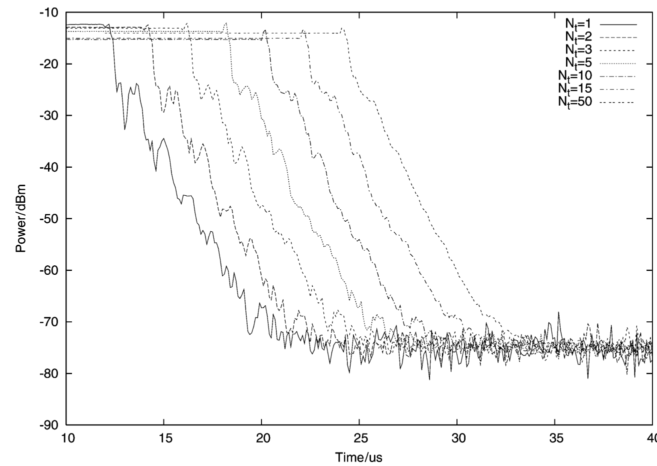

Fig. 3. Average traces for different numbers of tuner positions for a frequency of $f = 200$ MHz (near the LUF). Traces are shifted along the time axis for better distinction.

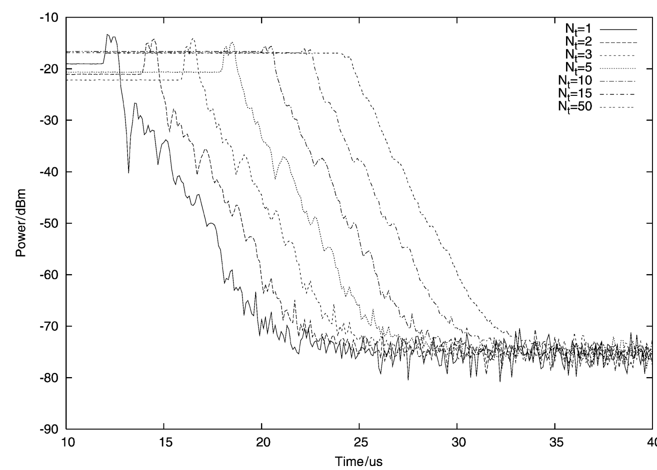

Fig. 4. Average traces for different numbers of tuner positions for a frequency of $f = 300$ MHz. Traces are shifted along the time axis for better distinction.

signal of the incoming wave is measured and displayed as a function of time for the given center frequency and resolution bandwidth (RBW). Thus, this is a band-limited time-domain measurement. The measurement of the quality factor in the time domain is well known from the literature, e.g., [11], [16], and [17]. The advantage of using a spectrum analyzer instead of an oscilloscope is that a bandwidth can be used that is just large enough to not affect the slope of the signals envelope. In turn, the bandwidth is small enough—even for very height carrier frequencies—to achieve a good signal-to-noise ratio. This allows for a simple and accurate measurement of the chamber time constant. From a practical point of view, it is also important to note that spectrum analyzers are already available in most EMC laboratories, in contrast to high-performance oscilloscopes.

The quality factor $\langle Q\rangle$ can be extracted directly from the linear-averaged trace measured with the spectrum analyzer [14], [15].

In the time domain, the quality factor is given by

$$\langle Q\rangle = \frac{\pi}{d} = 2\pi f \tau \tag{19}$$

where d is the average logarithmic decrement of the free-decay field of energy density stored in any point of the enclosure [11]

$$d = \frac{1}{f\,\Delta t} \ln\left(\frac{E(t_0)}{E(t_0+\Delta t)}\right) \tag{20}$$

$$= \frac{\ln(10)}{20 f\,\Delta t}\,\Delta E_{\mathrm{dB}} \tag{21}$$

$$= \frac{\ln(10)}{20 f\,\Delta t}\,\Delta P_{\mathrm{dB}}. \tag{22}$$

The energy (field) decay time constant τ is given by

$$\langle E(t_0+\tau)\rangle = \left(1/\sqrt{e}\right)\langle E(t_0)\rangle \tag{23}$$

$$\langle E_{\mathrm{dB}_{\mathrm{V/m}}}(t_0+\tau)\rangle = \langle E_{\mathrm{dB}_{\mathrm{V/m}}}(t_0)\rangle - 4.34\,\mathrm{dB}_{\mathrm{V/m}}. \tag{24}$$

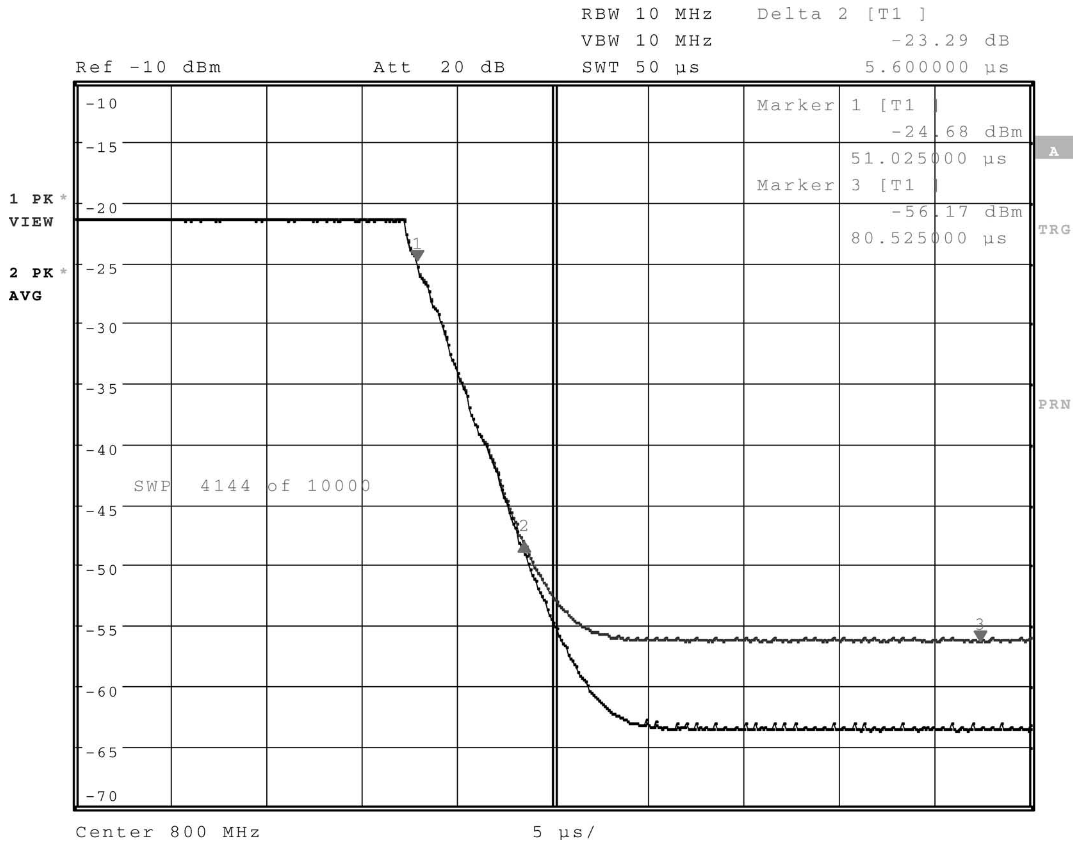

Fig. 5. Averaged traces showing the steady-state region ("On,SS"), the free energy decay ("Off,T"), and the "Off,SS" region. The higher power levels in the right part of one of the traces are due to the EUT radiation. For the other trace, the EUT was off. The slope in the transient region is not affected by the radiation of the EUT.

From (22) and (19), we obtain

$$\langle Q\rangle = \frac{20\pi f\,\Delta t}{\ln(10)\,\Delta P_r|_{\mathrm{dB}}} \approx 27.29\frac{f\,\Delta t}{\Delta P_r|_{\mathrm{dB}}}. \tag{25}$$

Typical traces for different tuner positions are shown in Fig. 2 along with the averaged trace. Figs. 3 and 4 present the average traces for different numbers of tuner positions ($N_t = 1,\ 2,\ 3,\ 5, 10,\ 15,\ 50$) for a frequency near the chamber lowest usable frequency (LUF) ($f = 200$ MHz) and a frequency well in the operating range of the chamber ($f = 300$ MHz).

In contrast to the incoming signal, three ranges of time have to be distinguished here. While the signal generator is on, a constant power level is recorded due to steady-state field conditions in the RC ("On,SS"). After the external signal gets off, a complex transient trace appears for several microseconds ("Off,T"). Finally, a new steady state is reached ("Off,SS").[2]

The free energy decay time τ will become shorter if the quality factor Q is reduced. Since the measurement is limited by the RBW of the receiver (the bandwidth of the receiving antenna is typically much larger), a lower Q limit will exist for the method. Below that limit, the slope would be too steep to be recorded correctly. To calculate this limit, the common relation between the 90–10% fall time and the bandwidth can be used: $T_{90,10} \geq 0.35/\mathrm{RBW}$. By using (20), we obtain

$$d = \frac{1}{fT_{90,10}}\ \ln\left(\frac{0.9E_0}{0.1E_0}\right) \tag{26}$$

$$= \frac{\mathrm{RBW}}{0.35f}\ \ln(9) \approx \frac{6.28\times\mathrm{RBW}}{f}. \tag{27}$$

This gives a theoretical lower limit for the quality factor

$$Q_{\mathrm{min,th}} = \frac{\pi}{d} \approx \frac{f}{2\times\mathrm{RBW}}. \tag{28}$$

For real use, the signal fall time should be larger than $T_{90,10}$ by a factor of 3–5. This leads to a real Q factor limit that is larger by a factor of 3–5

$$Q_{\mathrm{min,real}} = kQ_{\mathrm{min,th}} \qquad k \text{ between } 3 \text{ and } 5. \tag{29}$$

Using $k = 5$ yields a very good agreement with the experimental results presented in [15].

The evaluation of (25) is very simple. For the case of mode-stirred operation, the linear averaging of the traces could be done by the spectrum analyzer itself. Then, one can easily use the marker functions to obtain $\Delta t|_{\mu s}$ and $\Delta P_r|_{\mathrm{dB}}$ in order to calculate $\langle Q\rangle$.

[2]There is a second transient range after the external signal gets on again. This transient state is not considered here.

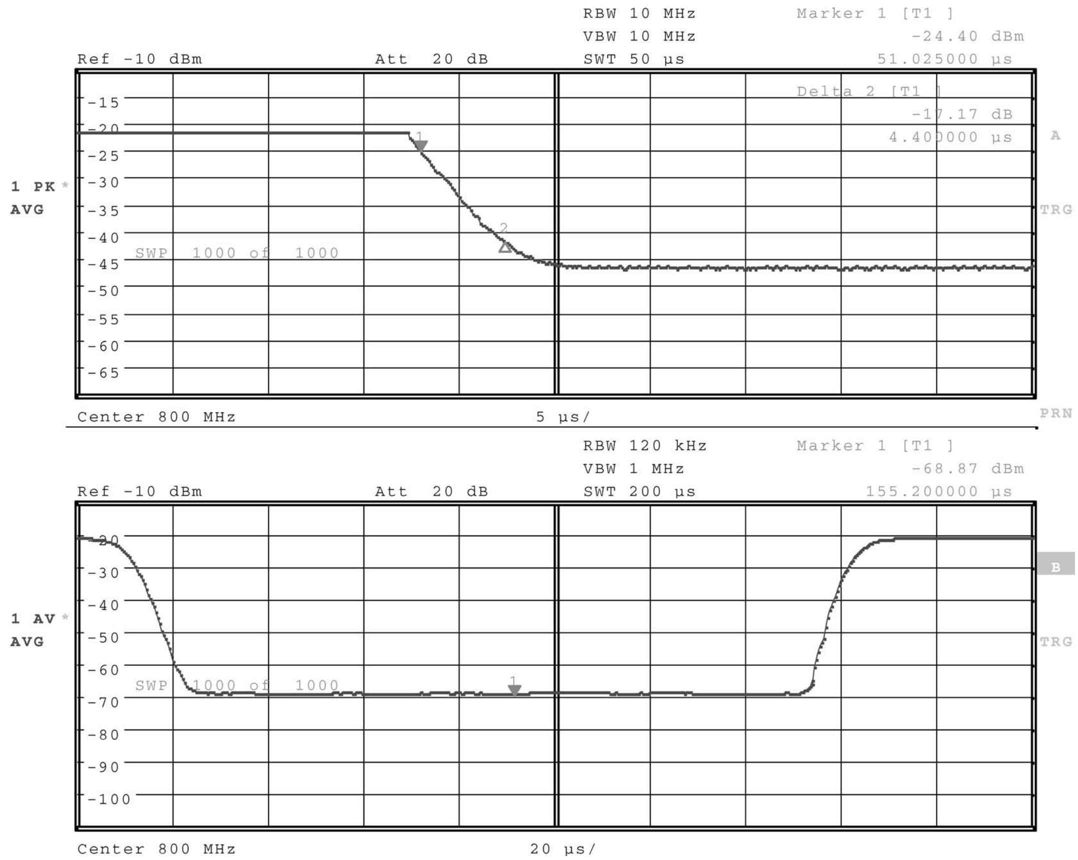

Fig. 6. Measurement of two (averaged) traces with different measurement parameters. The upper trace is used to determine the quality factor (peak detector, 10 MHz RBW). The lower trace is used to measure the radiation from the EUT with appropriate measurement parameters (here, average detector, 120 kHz RBW).

For the case of mode-tuned operation, the traces have to be saved and the average has to be evaluated in post processing. The evaluation "by hand" is then inconvenient—automation is the better solution.

2) Simultaneous Measurement of $\langle Q \rangle$ and $\langle P_r \rangle$: The power at the receiving antenna during the "On,SS" time is, or can be made to be much higher than the power only from the EUT. Thus, the same procedure to measure the quality factor described before can be used even if the EUT is radiating. As shown in Fig. 5, neither the steady-state level during the "On,SS" time, nor the slope of the free energy decay ("Off,T") will be affected significantly due to the presence of the radiating EUT compared to the case when the EUT is present but not radiating. Therefore, it is possible to obtain all information to evaluate (12), Δt, ΔP_r, and $\langle P_r \rangle$, from one single averaged trace. The values of Δt and ΔP_r are taken from the region of the free energy decay ("Off,T"), and $\langle P_r \rangle$ is the power level during the "Off,SS" time. Of course, this is true only if the emissions from the EUT are well-separated narrow-band signals. In this case, the measured power level will not be affected by the chosen RBW (typically 3–10 MHz). Generally, one has to select a certain combination of detector, RBW, and video bandwidth, which will be different from the one used to measure the free energy decay. This is not a real problem, since modern spectrum analyzers can measure and display two traces with different settings time interleaved (see Fig. 6). The doubling of the time to get the complete information is uncritical in most cases because the sweep time is of the order of several tenths of a microsecond.

The combination of (12) and (25) yields

$$\langle P_t \rangle = \frac{4\pi V \ \ln(10) f^2 \, \Delta P_{\mathrm{dB}}}{\eta_r 5 c^3 \, \Delta t} \langle P_r \rangle. \tag{30}$$

It may be convenient to convert this equation to decibel-scaled quantities[3]

$$\begin{aligned}\langle P_t \rangle|_{\mathrm{dB\,m}} = & - 10 \ \log(\eta_r) + 10 \ \log(V|_{\mathrm{m}^3}) \\ & - 10 \ \log(\Delta t|_{\mu\mathrm{s}}) + 20 \ \log(f|_{\mathrm{MHz}}) \\ & - 66.68 + 10 \ \log(\Delta P_{\mathrm{dB}}) + \langle P_r \rangle|_{\mathrm{dB\,m}}. \end{aligned} \tag{31}$$

For a given RC, $-10 \ \log(\eta_r) + 10 \ \log(V|_{\mathrm{m}^3}) - 66.68$ will result in a chamber-specific constant.

The sensitivity of the new measurement method can be evaluated by performing a measurement without an EUT being present, i.e., performing a noise measurement and evaluating the noise data as it would be an EUT. Results of such measurements for RBWs of 100 kHz and 1 MHz, and with an internal spectrum analyzer attenuation of 10 dB are depicted in Fig. 7. The noise level is determined by the equipment used and the measurement settings. Thus, it is not the subject of the method used (IEC versus new method). The noise level is presented

[3]The term $+10 \ \log(\Delta P_{\mathrm{dB}})$ may be error-prone. Take care to take 10 times the logarithm of the already decibel-scaled quantity.

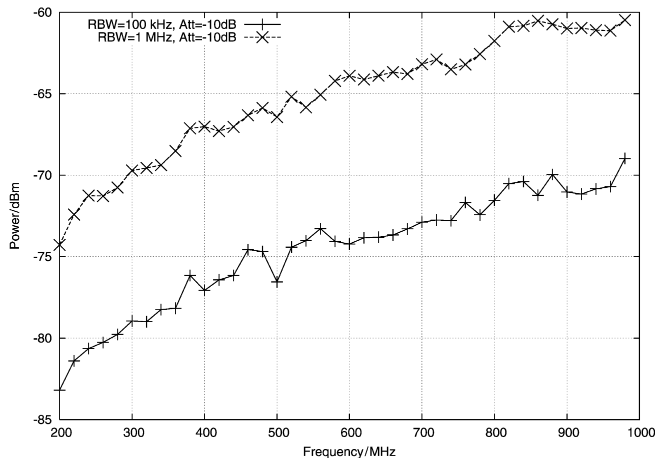

Fig. 7. Noise levels for two different settings of the spectrum analyzer RBW.

Fig. 8. Noise emitter CNEIII with the 100-mm top-loaded monopole antenna.

Fig. 9. Comb generator RSG2000 with the 100-mm top-loaded monopole antenna.

only to be compared to the measured levels of two EUTs given later.

III. Results

In order to evaluate the proposed method, two devices have been investigated. The first is a noise emitter CNEIII from York Electromagnetics that is used in conjunction with a 100-mm top-loaded monopole antenna. The antenna is specified for frequencies up to 1 GHz. The device with the mounted antenna is shown in Fig. 8.

The second device is a comb generator RSG2000 from Schaffner. The output power of that generator was attenuated by 20 dB. The same top-loaded monopole antenna as for the CNEIII was used for the emission measurements. The RSG2000 is shown in Fig. 9.

In any case, three different measurements have been performed. First, the generator output power was recorded using an FSP spectrum analyzer from Rohde & Schwarz. For the CNEIII, 100 kHz RBW and the average detector was used. For the RSG2000, the same bandwidth but the maximum peak detector was used. Second, an emission measurement according to IEC 61000-4-21 was performed with EUT calibration and EUT measurement. The total radiated power was calculated using the CCF and the CLF according to (13) and (15), respectively. Finally, the total radiated power was measured using the new method described in Section II-B. Here, two traces have been measured simultaneously. The free energy decay was measured with the maximum bandwidth of the spectrum analyzer (10 MHz). The EUT emission during the “Off,SS” time was recorded using the detector and bandwidth settings as in the IEC measurements.

All emission measurements have been performed in the large Magdeburg RC. The LUF of the chamber is 200 MHz.

A. Noise Emitter CNEIII

The noise generator CNEIII is designed to produce a pseudonoise signal with frequencies up to 2 GHz. In order to compare the results from the IEC method and the new method, the total radiated power has been measured in the frequency range from 200 MHz up to 1 GHz using 20-MHz steps.

The results are shown in Fig. 10. Comparing the measurements, a very good agreement is achieved for frequencies below 500 MHz and above 900 MHz. Between 500 and 900 MHz, the deviations are larger (up to 5 dB), but still satisfying for independent measurements on noisy signals. The remaining deviation is subject to further investigations.

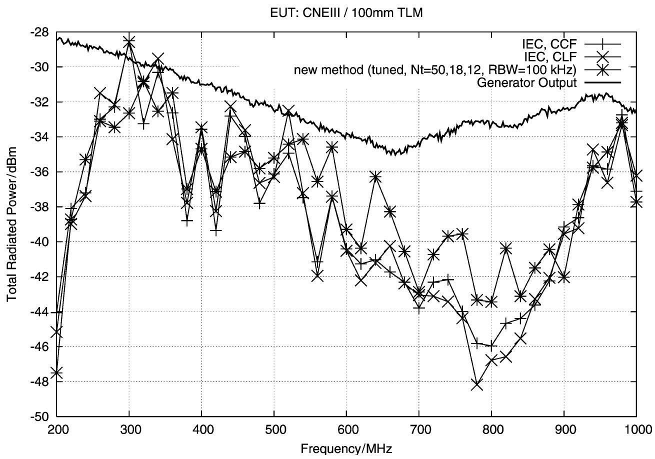

Fig. 10. Generator output power and total radiated power of the CNEIII noise emitter.

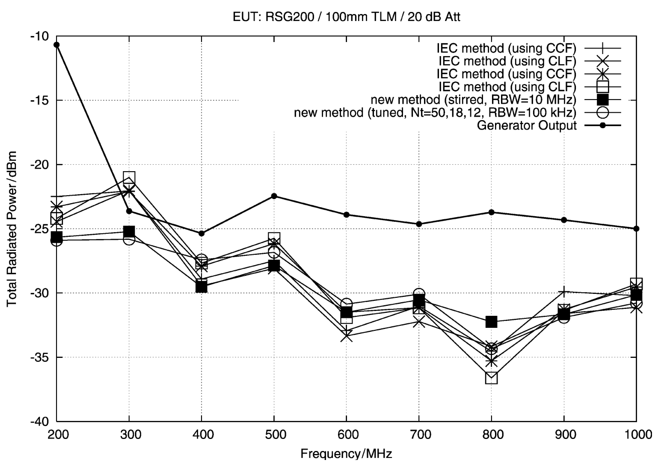

Fig. 11. Generator output power and total radiated power of the RSG2000.

B. Comb Generator RSG2000

The comb generator RSG2000 produces needle impulses with 100-MHz spacing for frequencies up to 18 GHz. So, there are only nine frequencies to measure in the range from 200 MHz (LUF of the chamber) up to 1 GHz (upper frequency of the monopole antenna).

The results of the measurements are shown in Fig. 11. For both methods (IEC and new method), two independent measurements were performed, in order to show the test–retest reproducibility of the measurements. Additionally, in the case of the new method, a first measurement was performed manually. In this case, the spectrum analyzer's built-in averaging functionality was used on the measured trace. In order to record the free energy decay correctly, the RBW was 10 MHz. This measurement was performed using mode-stirred operation of the chamber. The total radiated power was calculated manually from three trace markers using (31). The second measurement with the new method was remote controlled, and used two traces with different bandwidth settings for the free energy decay and the measurement of the EUT radiation. This measurement was performed using mode-tuned operation of the chamber

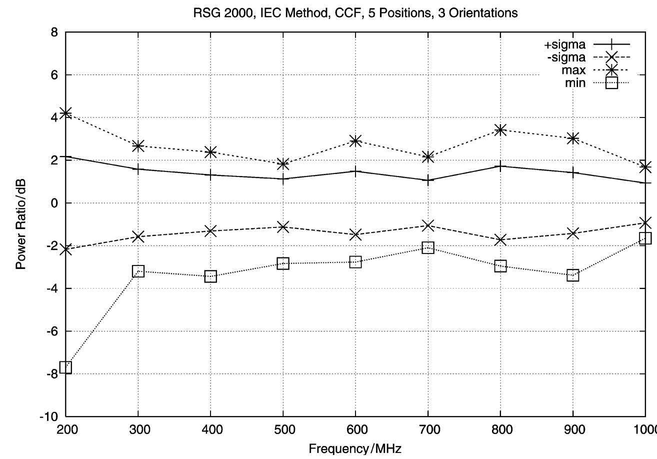

Fig. 12. Deviation from the average total radiated power for the IEC method using CCF. The measurements have been performed at five different positions and three orientations of the EUT. The four lines indicate the standard deviation ($\pm\sigma$) and the minimal (min) and maximal (max) results.

The measurement results of the methods among themselves are in good agreement. For the new method, the discrepancy of the results is less then 2.5 dB. The main reasons for the discrepancy are manual versus automated measurement and mode-stirred versus mode-tuned operation. In the case of the comb generator, the influence of the bandwidth is negligible. The deviation of the two IEC measurements is also less than 2.5 dB.

The intermethod comparison yields similar results. Only two frequencies are conspicuous: at 300 MHz, the IEC results are more than 3 dB higher, and at 800 MHz, the result from the manual measurements according to the new method is more than 2.5 dB higher than the other results.

The generator output power should be an upper limit for all measurements of the total radiated power. Nevertheless, this limit is exceeded at 300 MHz for two independent measurements according to the IEC standard. Since all four results of the IEC method (two measurements, two possible evaluations) are similar, and since only the evaluation with the CLF uses information from the main calibration, the cause of this effect has to be in the EUT calibration or in the EUT measurement. Up to now, the reason is not clear and the topic is subject to further investigations.

C. Evaluation for Different Positions in the Chamber

The excitation of an RC by a certain power will result in an inhomogeneous spacial distribution of field strength, energy density, (scalar) power density, and other quantities. The spacial variation depends on the number of independent boundaries realized, e.g., by the moving tuner. This can be understood as a position-dependent coupling between the transmitting antenna and the receiving antenna. Thus, field inhomogeneity is an intrinsic limiting parameter for the accuracy of both immunity and emission measurements in RC and is independent from the measurement method. It is, therefore, expected to obtain different

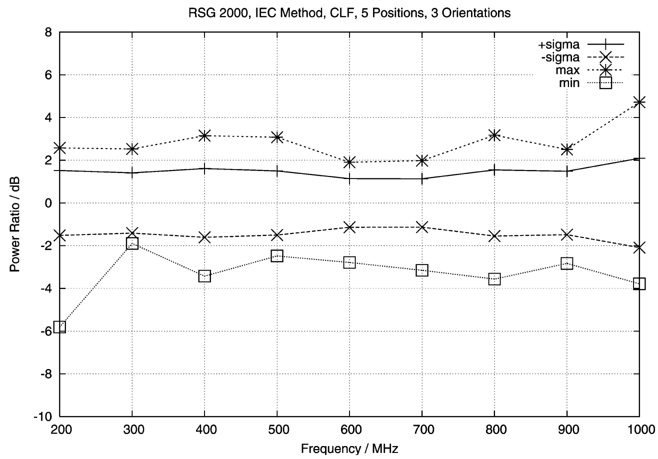

Fig. 13. Deviation from the average total radiated power for the IEC method using CLF. The measurements have been performed at five different positions and three orientations of the EUT. The four lines indicate the standard deviation ($\pm\sigma$) and the minimal (min) and maximal (max) results.

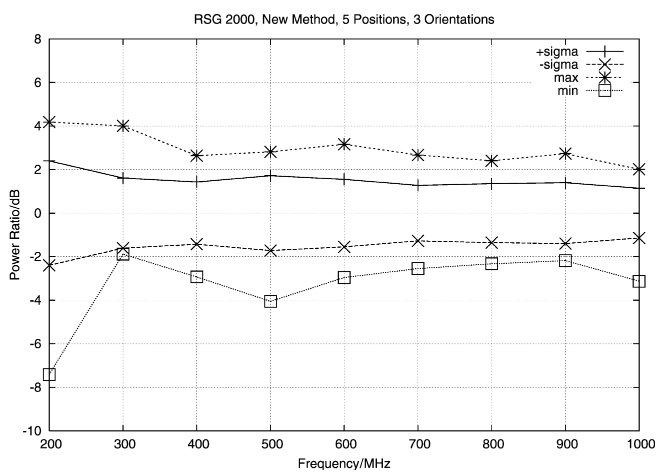

Fig. 14. Deviation from the average total radiated power for the new method. The measurements have been performed at five different positions and three orientations of the EUT. The four lines indicate the standard deviation ($\pm\sigma$) and the minimal (min) and maximal (max) results.

measurement results if the position of the EUT within the working volume of the chamber is changed. In order to evaluate the new method with respect to the two IEC methods, the emission measurements for the RSG2000 have been performed for five different positions and three different (orthogonal) orientations of the EUT for each method.

The results (with respect to the average of the 15 measurements) are presented in the Figures 12 (IEC method, CCF), 13 (IEC method, CLF), and 14 (new method).

As expected, there is no winner regarding the observed deviations. The standard deviation is in the range of ± 1.5 to ± 2 dB and minimal and maximal deviations are typically limited to ± 3 dB. For all methods, the magnitude of the minimal deviation is significantly larger (6–8 dB) for the lowest frequency (near the LUF).

Fig. 15. Comb generator RSG2000 with four blocks of absorbers to simulate an EUT with a higher chamber loading. A different loading was realized by using only the two absorber blocks on the table.

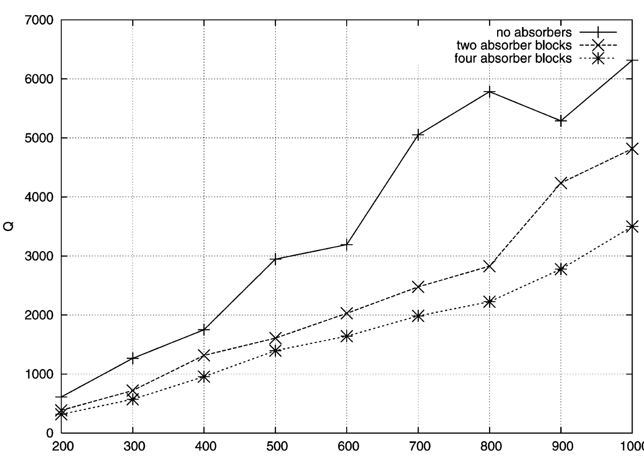

Fig. 16. Chamber quality factor Q of the chamber loaded by the EUT only, and with two and four additional absorber blocks.

D. Evaluation for Different Chamber Loading

Both EUTs used for the evaluation of the new method are small and do not load the chamber significantly. In order to simulate EUTs with a higher chamber loading, the emission measurements have also been performed with additional absorbers present near the RSG2000 comb generator. Thus, three different loadings have been realized: without absorbers, with two blocks of absorbers below the EUT, and with four blocks of absorbers. The configuration with four absorber blocks is shown

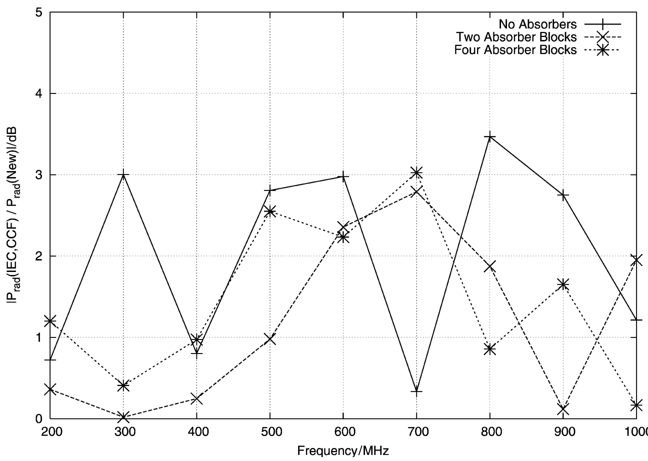

Fig. 17. Ratios of the radiated power of the IEC method (CCF) and the new method for three different EUT loadings.

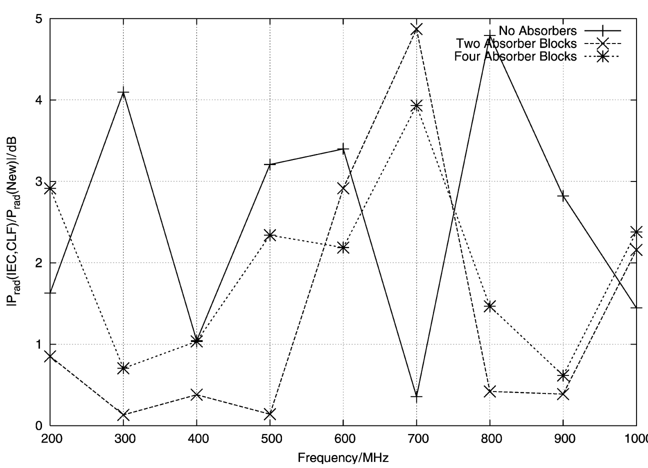

Fig. 18. Ratios of the radiated power of the IEC method (CLF) and the new method for three different EUT loadings.

in Fig. 15. The chamber quality factors for the three different loadings are given in Fig. 16.

The deviation between the IEC method using the CCF and the new method is found to be less than 3 dB (see Fig. 17). For the IEC method using the CLF versus the new method, the deviation is significantly larger (up to 5 dB) (see Fig. 18).

In order to judge the observed deviations, they can be compared to the deviation of the two IEC methods, the ratio of which is given in Fig. 19. Obviously, the deviation "IEC,CCF versus new method" is in the same range as the deviation "IEC, CCF versus IEC, CLF." Since the "IEC, CCF" method uses average power readings, and does not need information from the main calibration, it can be regarded as the more accurate of the two IEC methods (as long as the average power readings are well above the noise level). So, the accuracy of the new method with respect to the more accurate IEC methods (CCF) is better than the accuracy of the "IEC, CLF" method with respect to the "IEC, CCF" method.

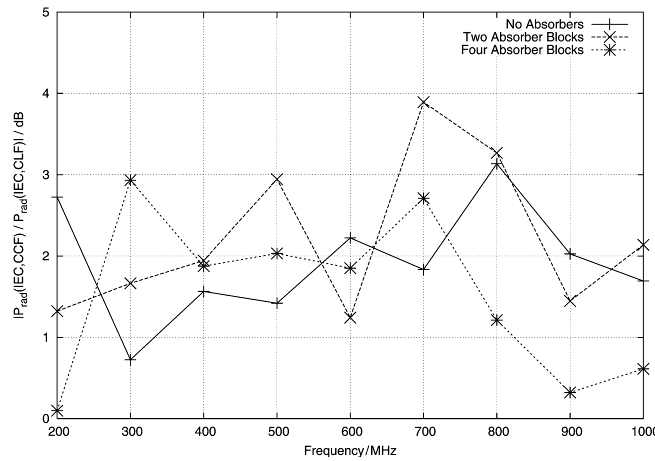

Fig. 19. Ratios of the radiated power of the two IEC methods (CCF and CLF) for three different EUT loadings.

IV. Conclusion

A new method to measure the total radiated power of EUTs in RCs has been introduced. The method is independent of the standard IEC method, but is based on the same principal formula. Experimental results have been presented for a noise emitter CNEIII and a comb generator RSG2000. In both cases, the agreement of the results is reasonably good. Additionally, the influence of the inhomogeneous field distribution on the measured total radiated power has been accounted for all methods. It has been shown that the uncertainty due to the field inhomogeneity is independent from the method used. Further, the validity of the new method in the case of additionally loading has been proven.

The main advantages of the new method are as follows.

1) No EUT calibration is required.
2) No information from the main chamber calibration is used.
3) The method is faster (due to the previous items).
4) The method is simpler.
5) In the case of the mode-stirred technique, the averaging can be performed with the spectrum analyzer directly.
6) Since no information from previous measurements is used, the overall uncertainty budget may be reduced (subject to further investigations).

References

[1] Joint Task Force IEC SC77B–CISPR/A, *Electromagnetic Compatibility (EMC)—Part 4.21: Testing and Measurement Techniques—Reverberation Chamber Test Methods*, IEC 61000-4-21. Geneva, Switzerland, Aug. 2003.

[2] C. L. Holloway, P. F. Wilson, G. Koepke, and M. Candidi, "Total radiated power limits for emission measurements in a reverberation chamber," in *Proc. 2003 IEEE Int. Symp. Electromagn. Compat.*, vol. 2, pp. 838–843.

[3] G. Koepke, D. Hill, and J. Ladbury, "Directivity of the test device in EMC measurements," in *Proc. 2000 IEEE Int. Symp. Electromagn. Compat.*, vol. 2, pp. 535–539.

[4] P. Wilson, G. Koepke, J. Ladbury, and C. L. Holloway, "Emission and immunity standards: Replacing field-at-a-distance measurements with total-radiated-power measurements," in *Proc. 2001 IEEE Int. Symp. Electromagn. Compat.*, vol. 2, pp. 964–969.

[5] P. F. Wilson, D. A. Hill, and C. L. Holloway, "On determining the maximum emissions from electrically large sources," *IEEE Trans. Electromagn. Compat.*, vol. 44, no. 1, pp. 79–86, Feb. 2002.

[6] P. Wilson, C. L. Holloway, and G. Koepke, "A review of dipole models for correlating emission measurements made at various EMC test facilities," in *Proc. 2004 Int. Symp. Electromagn. Compat.*, vol. 3, pp. 898–901.
[7] L. R. Arnaut, "Statistics of the quality factor of a rectangular reverberation chamber," *IEEE Trans. Electromagn. Compat.*, vol. 45, no. 1, pp. 61–76, Feb. 2003.
[8] J. Ladbury, G. Koepke, and D. Camell, "Evaluation of the NASA Langley Research Center mode-stirred chamber facility," NIST, Boulder, CO, NIST Tech. Note TN 1508, Jan. 1999.
[9] F. Borgnis and C. Papas, "Electromagnetic waveguides and resonators," in *Handbuch der Physik,* S. Flügge, Ed., vol. 16, Berlin, Germany: Springer-Verlag, 1958, pp. 285–422.
[10] D. A. Hill, "Plane wave integral representation for fields in reverberation chambers," *IEEE Trans. Electromagn. Compat.*, vol. 40, no. 3, pp. 209–217, Aug. 1998.
[11] P. Corona, G. Latmiral, and E. Paolini, "Performance and analysis of a reverberating enclosure with variable geometry," *IEEE Trans. Electromagn. Compat.*, vol. EMC-22, no. 1, pp. 2–5, Feb. 1980.
[12] D. A. Hill, M. L. Crawford, M. Kanda, and D. I. Wu, "Aperture coupling to a coaxial air line: Theory and experiment," *IEEE Trans. Electromagn. Compat.*, vol. 35, no. 1, pp. 69–74, Feb. 1993.
[13] M. Höijer, "Maximum power available to stress onto the critical component in the equipment under test when performing a radiated susceptibility test in the reverberation chamber," *IEEE Trans. Electromagn. Compat.*, vol. 48, no. 2, pp. 372–384, May 2006.
[14] H. G. Krauthäuser and J. Nitsch, "Transient fields in mode-stirred chambers," presented at the XXVIIth Gen. Assem. Int. Union Radio Sci. (URSI 2002). Maastricht, The Netherlands.
[15] H. G. Krauthäuser and J. Nitsch, "Effects of the variation of the excitation and boundary conditions of mode-stirred chambers and consequences for calibration and measurements," in *Proc. 15th Int. Zurich Symp. Tech. Exhib. Electromagn. Compat. 2003*. Zurich, Switzerland: Commun. Technol. Lab. Lab. Electromagn. Fields Microw. Electron. Swiss Federal Inst. Technol. Zurich, Feb., pp. 615–620.
[16] D. A. Hill, M. T. Ma, A. R. Ondrejka, B. F. Riddle, M. L. Crawford, and R. T. Johnk, "Aperture excitation of electrically large, lossy cavities," *IEEE Trans. Electromagn. Compat.*, vol. 36, no. 3, pp. 169–178, Aug. 1994.
[17] J. M. Ladbury, R. T. Johnk, and A. R. Ondrejka, "Rapid evaluation of mode-stirred chambers using impulsive waveforms," NIST, Boulder, CO, NIST Tech. Note 1381, Jun. 1996.

Hans Georg Krauthäuser (M'98) was born in Cologne, Germany, in 1965. He received the M.S. degree in physics and the Ph.D. degree in small-angle X-ray and neutron scattering of unordered mesoscopic systems and the solution of ill-posed inverse problems from the University of Cologne, Cologne, in 1992 and 1996, respectively, and the Postgraduate degree in medical physics and technology from the University of Kaiserslautern, Kaiserslautern, Germany, in 1996.

He is currently a Research Assistant at the Otto-von-Guericke University, Magdeburg, Germany, where he has been an Assistant Lecturer of electromagnetic compatibility measurement technology since 2002 and is engaged in the experimental laboratories of the Chair "Electromagnetic Compatibility and Theoretical Electrical Engineering." His current research interests include reverberation chambers, electromagnetic interactions with complex systems, measurement technology, and inverse scattering problems. He is the author or coauthor of more than 40 scientific papers published in peer-reviewed conference proceedings and journals.

Dr. Krauthäuser is a Member of the CISPR/A-IEC/SC77B Joint Task Force on Reverberation Chambers.